Current Biology 17, 1426–1431, August 21, 2007 ©2007 Elsevier Ltd All rights reserved DOI 10.1016/j.cub.2007.07.040

Report

Individual Differences in White-Matter Microstructure Reflect Variation in Functional Connectivity during Choice

Erie Dell Boorman,[1,2,3,*] Jacinta O'Shea,[1,2,3] Catherine Sebastian,[2] Matthew F.S. Rushworth,[1,2] and Heidi Johansen-Berg[1]
[1] Centre for Functional MRI of the Brain
University of Oxford
Oxford OX3 9DU
United Kingdom
[2] Dept of Experimental Psychology
University of Oxford
Oxford OX1 3UD
United Kingdom

Summary

The relation between brain structure and function is of fundamental importance in neuroscience. Comparisons between behavioral and brain-imaging measures suggest that variation in brain structure correlates with the presence of specific skills [1–3]. Behavioral measures, however, reflect the integrated function of multiple brain regions. Rather than behavior, a *physiological* index of function could be a more sensitive and informative measure with which to compare structural measures. Here, we test for a relationship between a physiological measure of functional connectivity between two brain areas during a simple decision-making task and a measure of structural connectivity. Paired-pulse transcranial magnetic stimulation indexed functional connectivity between two regions important for action choices: the premotor and motor cortex. Fractional anisotropy (FA), a marker of microstructural integrity, indexed structural connectivity. Individual differences in functional connectivity during action selection show highly specific correlations with FA in localized regions of white-matter interconnecting regions, including the premotor and motor cortex. Probabilistic tractography [4, 5], a technique for identifying fiber pathways from diffusion-weighted imaging (DWI), was used to reconstruct the anatomical networks linking the component brain regions involved in making decisions. These findings demonstrate a relationship between individual differences in functional and structural connectivity within human brain networks central to action choice.

Results

We employed a novel strategy to test whether a physiological index of functional interactions between brain regions important for action selection correlates with the microstructural integrity of specific white-matter pathways. Because convergent neurophysiological [6, 7], neuroimaging [8–11], and single-pulse transcranial magnetic stimulation (TMS) [8, 12, 13] evidence has implicated interactions between the dorsal premotor cortex (PMd) and the primary motor cortex (M1) in the process of externally cued action selection, we focused our investigation on these two regions. We first assessed functional connectivity between the PMd and M1 during a particular cognitive state—action selection. We then tested for an association between this measure of functional connectivity and fractional anisotropy (FA) values calculated within a white-matter network.

Physiological Results Measured by Paired-Pulse TMS

One physiological approach to measuring functional connectivity is paired-pulse TMS. In the paired-pulse-TMS protocol we use here, a test pulse over the M1 is preceded by a conditioning pulse over the contralateral PMd at various interpulse intervals (IPIs) (Figure 1A). The conditioning pulse modulates the amplitude of motor-evoked potentials (MEPs) elicited by the test pulse, depending on the IPI at which the conditioning pulse is delivered [14–16]; this technique has therefore been taken as a measure of functional connectivity between stimulated regions [17].

Recently, paired-pulse TMS has been used to assess functional connectivity between the PMd and contralateral M1 during action selection [18, 19]. In a previous experiment, we assessed functional connectivity during an action selection ("choice") task. In this task, subjects selected left- or right-index-finger responses on the basis of four learned visuomotor associations (Figure 1B). We recorded MEP amplitudes from the first dorsal interosseous (FDI) hand muscle contralateral to the stimulated M1 when M1 test pulses were preceded by conditioning pulses over the contralateral PMd by an 8 ms IPI [14, 16]. In a second condition, we reversed the TMS coils so that both lPMd-rM1 and rPMd-lM1 combinations were tested. The TMS data are reported in full elsewhere [19]. Here, we wished to test how inter-individual variation in a specific TMS measure covaried with brain structure. The choice of TMS measure was motivated by the results of our previous study. In brief, MEP amplitudes were significantly facilitated by conditioning pulses at visual stimulus- (to TMS) onset asynchronies (SOAs) of 75 ms, as reported previously [18] (Figure 1C), interaction between SOA and TMS [$F(4,32) = 2.854$, $p = 0.039$], and corrected post-hoc paired-sample t tests for paired- versus single-pulse MEPs at 75 ms [$t(8) = -2.513$, $p = 0.036$]. Such facilitatory TMS effects are not directly related in a simple way to the increases in blood oxygenation levels that are measured with functional magnetic resonance imaging. Nevertheless, they likely reflect the coactivation of the PMd and M1 during action selection that has been demonstrated to occur in such tasks [10, 11, 13]. Moreover, this effect specific to action selection; modulation was absent at 75 ms in a simple movement-execution task for which subjects did not have to choose between

*Correspondence: erie.boorman@psy.ox.ac.uk
[3] These authors contributed equally to the project.

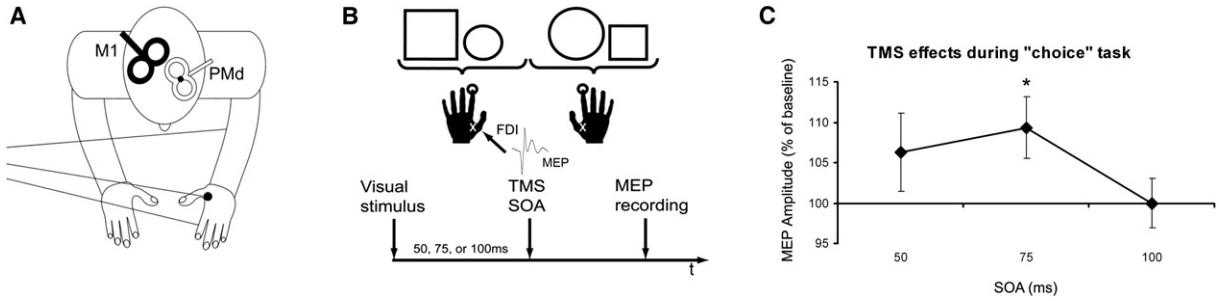

Figure 1. TMS Experimental Setup and Results

(A) Conditioning pulses were applied over the PMd and test pulses over the contralateral M1. In this example, coils are positioned over the lPMd and rM1. We tested both lPMd-rM1 and rPMd-lM1. MEPs were recorded from active electrodes over the FDI hand muscle (indicated by the black circle) contralateral to the stimulated M1.

(B) During the choice task, one of four shape stimuli was presented on each trial, and it remained on the screen until subjects made a button-press response with the index finger of the right or left hand (circled) according to a learned rule. TMS was delivered at SOAs of 50, 75, or 100 ms after the onset of the visual stimulus. On single-pulse TMS trials, a single TMS pulse was applied to the M1; on paired-pulse TMS trials, a conditioning TMS pulse was applied over the contralateral PMd 8 ms prior to the M1 pulse while motor-evoked potentials (MEPs) were recorded. Redrawn from [19].

(C) Effects during behavioral choice: normalized-mean-amplitude MEPs recorded from the FDI muscle contralateral to the stimulated M1. Error bars represent ± standard error of the mean (SEM). Redrawn from [19].

movements. fMRI studies similarly show that the premotor cortex is significantly less active in such control tasks [8, 10, 11, 13, 19, 20].

To capture this specific facilitatory effect at 75 ms during the choice task, we first calculated an MEP amplitude ratio between paired and single pulses and then calculated the difference between MEP ratios at SOAs of 75 ms and 100 ms (see Experimental Procedures). We also repeated these analyses with the MEP ratio between paired and single pulses at 75 ms only. We predicted positive correlations between TMS effects and FA, reflecting increasing FA associated with increasing functional connectivity.

Correlations between TMS Measures of Functional Connectivity and FA

Microstructural properties of human white matter can be interrogated in vivo with diffusion-weighted imaging (DWI), which is sensitive to apparent water-diffusion properties in brain tissue [21]. DWI takes advantage of the fact that water diffusion is orientation-dependent within tissue characterized by a high degree of directional organization, such as white matter. The orientational dependence of this diffusion can be quantified by *fractional anisotropy* at each voxel [22–24]. FA has been shown to reflect functionally relevant microstructural properties of white matter, including the axonal architecture, the extent of myelination, and the density of axonal fibers comprising axonal bundles [21], and has therefore been interpreted as a measure of microstructural integrity [25, 26].

To test whether there was a relationship between functional connectivity and white-matter microstructure across subjects, we used tract-based spatial statistics (TBSS) [27] to test for local correlations between FA estimates and TMS effect sizes (see Experimental Procedures). Because we were stimulating over the PMd and M1 and investigating correlates of action-selection signals, this analysis was restricted to a volume of interest (VOI) from a central portion of the brain predicted to mediate these effects.

In both conditions (lPMd-rM1 and rPMd-lM1) of our choice task, TMS-assessed functional connectivity was positively correlated with FA in white-matter tracts connecting premotor-parietal networks. Our multiple regression analysis revealed positive correlations between lPMd-rM1 functional connectivity and FA in clusters underlying the lPMd, rPMd, left sensorimotor cortex, and right superior longitudinal fascicle (SLF) ($t > 3.35$, $p < 0.005$; Figure 2, Table S1 in the Supplemental Data available online). Functional connectivity between the rPMd and lM1 was positively correlated with FA in clusters underlying the rPMd, bilateral premotor areas extending into supplementary motor areas (SMAs), the corpus callosum (CC), right SLF, and left inferior longitudinal fascile (ILF) ($t > 3.35$, $p < 0.005$; Figure 3, Table S1). The use of the MEP ratio at 75 ms only as the regressor for the TBSS analyses yielded virtually identical correlations (Figures S1 and S2). Note that within the restricted VOI used for the TBSS analysis, less than 0.5% of white-matter skeleton voxels were identified as significant, so these correlations were highly specific. When we repeated these analyses across the whole brain, we found additional correlations restricted to the SLF, extensions of the SLF in the posterior parietal cortex, the genu and splenium of the CC, the uncinate, and an anteroposterior tract bordering the forceps major (Table S1). Notably, the disconnection of the temporal and frontal lobes by uncinate transection in nonhuman primates induces a profound impairment in selecting between motor responses on the basis of a visual cue [28], indicating that this fascicle is functionally related to the choice task used here. It is important to note that FA in subregions of the same tract, interconnected tracts, or functionally related networks is likely to covary, and so these additional correlations might result from interregional white-matter correlations within the same tract or network, as previously reported for interconnected gray-matter regions [29, 30]. However, the use of a regressor derived from the PMd-M1 MEP modulation ratio at 100 ms (Figure 1C) yielded FA correlations restricted to the corticospinal tracts, and not in premotor

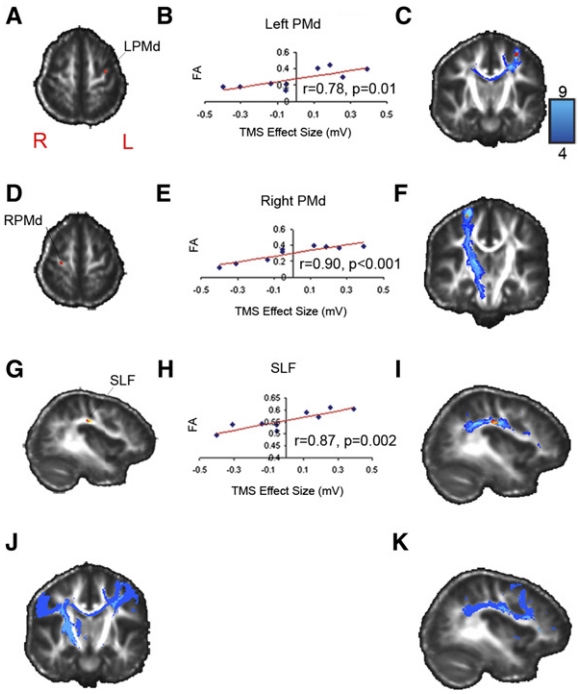

Figure 2. Local Correlations between FA and Functional Connectivity between the lPMd and rM1 during the Choice Task, and Probabilistic Tractography from Local Areas of Correlation

(A, D, and G): Clusters showing significant positive correlations between TMS effect sizes and FA when conditioning pulses were applied over the lPMd and test pulses over the rM1, overlaid on the mean FA image from all participants. The t statistic images are thresholded at $t > 3.35$ and cluster extent ≥ 10 voxels. Suprathreshold clusters are then dilated by one voxel for improved visualization. The color scale represents the t score from low (t = 3.35, red) to high (yellow). Images are displayed according to radiological convention.

(B, E, and H): Scatterplots showing individual FA and TMS values for selected clusters.

(C, F, I, J, and K): Group probability maps of tracts generated by PDT from positively correlated clusters when stimulating over lPMd-rM1. Maps were overlaid onto the mean FA image from all participants, and paths were color-coded according to whether the number of subjects containing that path is high (light blue) or low (dark blue).

An axial section illustrating correlation in white matter underlying the lPMd (labeled LPMd) (A), a scatterplot of individual FA values from the lPMd cluster shown in (A) and TMS values (B), and local premotor and transcallosal tracts generated from the lPMd cluster (C) are shown. An axial section of correlations in white matter underlying the rPMd (labeled RPMd) (D), a scatterplot of FA and TMS values from the rPMd cluster (E), and local premotor and CST tracts traced by PDT from the rPMd cluster (F) are shown. A sagittal section of the SLF correlated cluster (G), a scatterplot of FA and TMS values from the SLF cluster (H), and the SLF tract projecting from posterior parietal cortex to the PMd generated from the SLF cluster (I) are shown. In (J) and (K), a group probability map displaying the combined network of thresholded and summed tracts generated by PDT from all voxels within positively correlated clusters when stimulating over lPMd-rM1, shown in coronal section and sagittal sections, is presented.

white matter, the CC, or the SLF. This analysis demonstrates that at the 75 ms time point, PMd-M1 MEP modulation that is specifically related to the process of action selection is selectively associated with FA in the premotor cortex and its interconnecting fascicles. The correlations reported above all remained significant ($r > 0.78$, $p < 0.05$) after controlling for age, TMS stimulation intensities for both hemispheres, and skull-cortex distance (see Supplemental Data for further details).

Tractography from White-Matter Regions Showing Local Correlations

To elucidate the white-matter tracts in which local regions of FA correlation were found and the gray-matter targets to which they projected, we used these correlated clusters as seed masks for multifiber probabilistic diffusion tractography (PDT) [4, 31].

In the lPMd-rM1 condition, the correlated cluster underlying the lPMd generated local premotor and transcallosal paths to white matter underlying the contralateral PMd (Figure 2C). Conversely, the cluster underlying the rPMd was traced locally within the premotor cortex, but also inferiorly along the right corticospinal tract (CST), and did not branch into the CC (Figure 2F). The two clusters in the SLF generated paths between the posterior parietal and premotor cortex (Figure 2I). Finally, the sensorimotor cluster generated local paths between the sensorimotor and premotor cortex. This combined parietal-premotor-contralateral-premotor network of connectivity is illustrated in Figures 2J and 2K.

In the rPMd-lM1 condition, the correlated cluster underlying the rPMd also generated local premotor, transcallosal, and right CST paths (Figure 3C). Tractography from the additional clusters underlying premotor areas generated transcallosal tracts targeting homologous regions in the contralateral hemisphere, and the CC cluster generated both transcallosal paths targeting bilateral SMA and left CST paths (Figure 3F). Finally, the SLF cluster was traced between the parietal and premotor and prefrontal cortex (Figure 3I). This parietal-premotor-contralateral-premotor network of structural connectivity is shown in Figures 3J and 3K.

Note that our method for visualization of tracts (Figures 2 and 3) indicates the maximum number of subjects in whom a tract overlaps at each voxel in standard space and thereby provides a conservative estimate of intersubject consistency. For example, the maximum overlap of transcallosal tracts from the left PMd cluster shown in Figure 2A indicates that five out of nine subjects overlap at 2, −10, 25, whereas inspection of individual-subject tract maps reveals that from the left PMd cluster, transcallosal tracts are generated in seven out of nine subjects.

Discussion

We have demonstrated a correlation between natural variation in choice behavior-specific functional connectivity from the PMd to the contralateral M1 and the microstructural integrity of the specific white-matter networks presumed to mediate the physiological effects. The spatial specificity and replicability of the white-matter regions showing high correlation in the current study confirms that variation in white-matter structure across individuals is associated with variation in function in the same neural system. Such structural-physiological relationships might explain previous reports of correlation between brain structure and behavior [1–3, 32, 33].

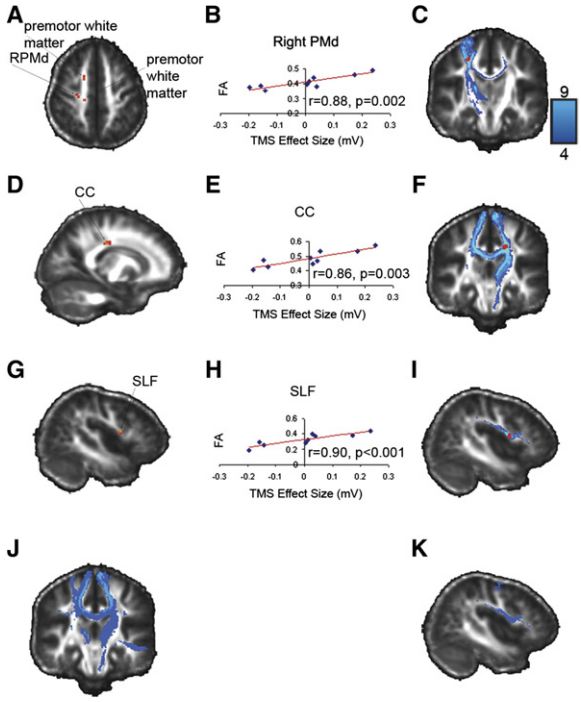

Figure 3. Local Correlations between FA and Functional Connectivity between the rPMd and lM1 during Action Selection and Probabilistic Tractography from Local Areas of Correlation

Images were produced and displayed with the same methods as in Figure 2.

(A–C) An axial section illustrating correlations in premotor white matter including white matter underlying the rPMd (labeled RPMd) and other premotor regions (A), a scatterplot between FA and TMS values (B), and tractography showing local premotor, transcallosal, and corticospinal paths (C).

(D–F) A sagittal section of the CC cluster (D), a scatterplot of FA and TMS values (E), and callosal paths targeting the SMA and a left CST path (F) generated by PDT.

(G–I) A sagittal section of the SLF correlation (G), a scatterplot between FA and TMS values (H), and the SLF tract coursing between the posterior parietal and prefrontal cortex (I).

(J and K) Coronal and sagittal sections of the group probability map, generated by thresholding and summing all tracts generated by PDT, illustrating a combined network of connectivity.

Our choice task and similar paradigms have previously been shown to recruit a premotor-parietal network with bilateral activations in the PMd and along the intraparietal sulcus (IPS) [8, 10, 11, 13, 20]. We found that TMS-assessed functional connectivity during the choice task correlated with FA specifically in the precentral gyrus white matter, possibly at the boundary between white and gray matter, underlying the conditioned PMd, the adjacent SLF connecting the IPS and premotor cortex and/or frontal pars opercularis, and the corpus callosum [34]. We also found correlations in white matter underlying premotor areas that extended to the bilateral SMA and sensorimotor cortex, consistent with the finding that blood-oxygen-level-dependent (BOLD) responses during the same choice task extend into these cortical regions [8, 10, 11, 13, 20]. Our physiological probe of FA therefore identified correlations in specific corticocortical tracts predicted by previous neuroimaging studies.

It is important to note, however, that within an individual, FA will vary along a tract because of factors such as fiber complexity and compression. Therefore, sensitivity to FA-physiology correlations might vary at different points along a tract. Thus, it is conceivable that the true extent of pathways involved in this task might be underestimated here.

FA is sensitive to multiple microstructural properties of white matter, including axon density, myelination, and possibly diameter [21, 35]. The functional connectivity-FA correlations we found might be caused by variation in axon density or diameter. Both electromyography (EMG) amplitude and area increase with fiber density in physiological studies of peripheral nerves, and with both fiber density and axon diameter in computer simulations [36, 37]. It is also possible that increased myelination or axon diameter across individuals led to increased or more-synchronized axonal conduction velocities, affecting the degree of interregional modulation observed.

The electrical conductivity and water self-diffusion tensors are closely related [38, 39], because some of the same geometric tissue properties that lead to increased anisotropic diffusion also lead to increased anisotropic conductivity. It is therefore possible that FA influences passive propagation of the TMS pulse. However, it is widely held that at the intensities used here, TMS excites cortical neurons and interneurons, generating descending volleys *trans*-synaptically, and not at the level of the axon itself [40]. In addition, the specific latency at which MEP modulation occurred strongly suggests that the PMd was functionally interacting with the contralateral M1 at this SOA. It is also important to note that we specifically controlled for stimulation thresholds over both hemispheres and skull-cortex distance. Taken together, these points suggest that the correlations we observed were predominately due to a relation between PMd-M1 physiological interactions and FA.

It is imperative to recall that our physiological measures are always of *relative* MEP modulation, rather than absolute MEP amplitudes. Variability in absolute physiological measures might be confounded with variability in distance between the TMS coil and precise brain region even after the scalp to brain surface has been considered. The relative modulation measure, for which coil position did not change between the SOAs, might be particularly suitable for comparing against a structural-connectivity measure.

With a cross-sectional study, it is not possible to determine the direction of causality between brain structure and function. Innate variation in structural connectivity of the motor system might determine the physiological measure recorded. Alternatively, variation in experience might induce functional plasticity in these motor pathways, which in turn results in measurable structural changes. Animal studies [41] and in vitro experiments [42] suggest that axonal size and myelination, which are known to modulate FA values [21], might be susceptible to experience-dependent change. Therefore, it is conceivable that variation in experience could result in variation in FA, a conclusion supported by evidence of correlations between FA and hours of musical training experienced by pianists [2]. Future

studies could test whether prolonged stimulation of a specific brain pathway, either behaviorally or physiologically, results in both functional and structural plasticity.

The current findings show that regionally specific microstructural features are related to physiological connectivity indices in human subjects during behavior. Such structural-physiological relationships might underlie recently reported individual differences in brain structure and behavior [1–3, 32, 33]. Our approach could be applied to clinical populations, for instance, to help characterize the extent of both the functional and anatomical reorganization that occurs in response to brain injury or stroke. The present results also suggest that FA could be related to other physiological measures, such as event-related potentials, to further investigate the relationship between the microstructural integrity of specific anatomical pathways and physiological indices of function.

Experimental Procedures

Subjects

Ten healthy, right-handed adults (three males, ages 23–32) underwent diffusion tensor imaging (DTI). Two subjects failed to complete one TMS condition (lPMd-rM1 or rPMd-lM1), resulting in nine subjects per TMS condition. Written informed consent was obtained for all subjects prior to participation, in accordance with local ethical approval.

TMS Analysis

The TMS methods are reported in full elsewhere [19] (see the Supplemental Experimental Procedures for details).

DWI and TBSS

We acquired diffusion-weighted (two acquisitions of 60 directions, b value 1000 s/mm^2, 2.5 × 2.5 × 2.5 mm^3 voxels, 60 slices) and T1-weighted data with a 1.5T Siemens Sonata MR scanner. Image analysis was carried out and FA values were calculated with Oxford Centre for Functional MRI of the Brain's (FMRIB's) diffusion toolbox (FDT) from FMRIB's Software Library (www.fmrib.ox.ac.uk/fsl). To test for correlations between TMS effect sizes and FA values, we employed tract-based spatial statistics (TBSS) [27], which enables statistical comparison of FA values from homologous regions of the FA map across subjects (see the Supplemental Experimental Procedures for details).

Correlation with TMS

To test whether there was a relationship between functional connectivity and FA values across subjects, we calculated the difference in MEP ratio between SOAs of 75 and 100 ms (i.e., MEPratio$_{75\ ms}$–MEPratio$_{100\ ms}$) and used this as a regressor in our TBSS analysis for both conditions. A general linear model (GLM) approach was used to correlate the TMS effect size for both conditions separately with FA values derived from the group skeleton. We restricted our analyses to the white matter within a central portion of the brain by using a probabilistic tissue-type segmentation of the MNI152 template brain, thresholded to include only those voxels classified as white matter in at least one-third of the population, and lying between y = 15 and y = −25. Having defined this restricted volume of interest and predicted positive correlations, we used a one-tailed statistical threshold $t > 3.35$ ($p < 0.005$ uncorrected) and a cluster extent threshold of ≥ 10 voxels.

Probabilistic Diffusion Tractography

Correlated clusters identified with TBSS above were then used as seed masks for PDT [4]. PDT estimates a probability distribution function (pdf) on fiber direction at each voxel. A multifiber model was fit to the diffusion data at each voxel, allowing for the tracing of fibers through regions of fiber crossing or complexity [31]. These methods are fully described elsewhere [4, 31]. Although this model is sufficient to resolve two crossing fibers with the parameters used here, higher field strengths, b values, and/or more diffusion directions would be necessary to resolve multiple fiber populations of three or more crossing fibers [19, 31]. Here, we drew 25,000 streamline samples from our seeded voxels through these pdfs to form an estimate of the probability distribution of connections from each seeded voxel. When these streamlines reach a voxel in which more than one direction is estimated, they follow the direction that is closest to parallel with the direction at which the streamline arrives. Tracts generated by PDT are volumes wherein values at each voxel represent the number of samples (or streamlines) that passed through that voxel. For the elimination of spurious connections, tractography in individual subjects was thresholded to include only voxels through which at least 50 samples had passed (out of 25,000). These individual tracts were then binarized and summed across subjects to produce group probability maps for each pathway. In these maps, each voxel value represents the number of subjects in whom the pathway passes through that voxel. For visualization, these group probability maps were then thresholded to display only those paths that were present in a minimum of ∼40% and a maximum of 100% of subjects. Those thresholded group probability maps from significant clusters were then summed to construct a composite connectivity network.

Supplemental Data

Experimental Procedures, two figures, and one table are available at http://www.current-biology.com/cgi/content/full/17/16/1426/DC1/.

Acknowledgments

We are grateful for financial support from the Wellcome Trust (E.D.B. and H.J.B.), the MRC and Royal Society (M.F.S.R.), and the Stevenson Junior Research Fellowship, University College Oxford (J.O.S.). We wish to thank T.E.J. Behrens for producing the tractography algorithm and for helpful comments and S.M. Smith and S. Jbabdi for help with TBSS analysis. E.D.B. and J.O.S. collected TMS data. J.O.S. analyzed TMS data. E.D.B. collected and analyzed diffusion-weighted image data.

Received: March 21, 2007
Revised: July 17, 2007
Accepted: July 18, 2007
Published online: August 9, 2007

References

1. Maguire, E.A., Gadian, D.G., Johnsrude, I.S., Good, C.D., Ashburner, J., Frackowiak, R.S., and Frith, C.D. (2000). Navigation-related structural change in the hippocampi of taxi drivers. Proc. Natl. Acad. Sci. USA *97*, 4398–4403.
2. Bengtsson, S.L., Nagy, Z., Skare, S., Forsman, L., Forssberg, H., and Ullen, F. (2005). Extensive piano practicing has regionally specific effects on white matter development. Nat. Neurosci. *8*, 1148–1150.
3. Gaser, C., and Schlaug, G. (2003). Brain structures differ between musicians and non-musicians. J. Neurosci. *23*, 9240–9245.
4. Behrens, T.E., Woolrich, M.W., Jenkinson, M., Johansen-Berg, H., Nunes, R.G., Clare, S., Matthews, P.M., Brady, J.M., and Smith, S.M. (2003). Characterization and propagation of uncertainty in diffusion-weighted MR imaging. Magn. Reson. Med. *50*, 1077–1088.
5. Behrens, T.E., Johansen-Berg, H., Woolrich, M.W., Smith, S.M., Wheeler-Kingshott, C.A., Boulby, P.A., Barker, G.J., Sillery, E.L., Sheehan, K., Ciccarelli, O., et al. (2003). Non-invasive mapping of connections between human thalamus and cortex using diffusion imaging. Nat. Neurosci. *6*, 750–757.
6. Cisek, P., and Kalaska, J.F. (2005). Neural correlates of reaching decisions in dorsal premotor cortex: Specification of multiple direction choices and final selection of action. Neuron *45*, 801–814.
7. Wise, S.P., Boussaoud, D., Johnson, P.B., and Caminiti, R. (1997). Premotor and parietal cortex: Corticocortical

connectivity and combinatorial computations. Annu. Rev. Neurosci. *20*, 25–42.

8. Johansen-Berg, H., Rushworth, M.F., Bogdanovic, M.D., Kischka, U., Wimalaratna, S., and Matthews, P.M. (2002). The role of ipsilateral premotor cortex in hand movement after stroke. Proc. Natl. Acad. Sci. USA *99*, 14518–14523.
9. Schluter, N.D., Rushworth, M.F., Mills, K.R., and Passingham, R.E. (1999). Signal-, set-, and movement-related activity in the human premotor cortex. Neuropsychologia *37*, 233–243.
10. Amiez, C., Kostopoulos, P., Champod, A.S., and Petrides, M. (2006). Local morphology predicts functional organization of the dorsal premotor region in the human brain. J. Neurosci. *26*, 2724–2731.
11. Grol, M.J., de Lange, F.P., Verstraten, F.A., Passingham, R.E., and Toni, I. (2006). Cerebral changes during performance of overlearned arbitrary visuomotor associations. J. Neurosci. *26*, 117–125.
12. Schluter, N.D., Rushworth, M.F., Passingham, R.E., and Mills, K.R. (1998). Temporary interference in human lateral premotor cortex suggests dominance for the selection of movements. A study using transcranial magnetic stimulation. Brain *121*, 785–799.
13. Rushworth, M.F., Johansen-Berg, H., Gobel, S.M., and Devlin, J.T. (2003). The left parietal and premotor cortices: Motor attention and selection. Neuroimage *20* (*Suppl 1*), S89–S100.
14. Mochizuki, H., Huang, Y.Z., and Rothwell, J.C. (2004). Interhemispheric interaction between human dorsal premotor and contralateral primary motor cortex. J. Physiol. *561*, 331–338.
15. Baumer, T., Bock, F., Koch, G., Lange, R., Rothwell, J.C., Siebner, H.R., and Munchau, A. (2006). Magnetic stimulation of human premotor or motor cortex produces interhemispheric facilitation through distinct pathways. J. Physiol. *572*, 857–868.
16. Koch, G., Franca, M., Mochizuki, H., Marconi, B., Caltagirone, C., and Rothwell, J.C. (2007). Interactions between pairs of transcranial magnetic stimuli over the human left dorsal premotor cortex differ from those seen in primary motor cortex. J. Physiol. *578*, 551–562.
17. Baumer, T., Rothwell, J.C., and Munchau, A. (2003). Functional connectivity of the human premotor and motor cortex explored with TMS. Suppl. Clin. Neurophysiol. *56*, 160–169.
18. Koch, G., Franca, M., Del Olmo, M.F., Cheeran, B., Milton, R., Alvarez Sauco, M., and Rothwell, J.C. (2006). Time course of functional connectivity between dorsal premotor and contralateral motor cortex during movement selection. J. Neurosci. *26*, 7452–7459.
19. O'Shea, J., Sebastian, C., Boorman, E.D., Johansen-Berg, H., and Rushworth, M.F.S. Functional specificity of dorsal premotor/motor cortical interactions during action selection. Eur. J. Neurosci., in press.
20. O'Shea, J., Johansen-Berg, H., Trief, D., Gobel, S., and Rushworth, M.F. (2007). Functionally specific reorganization in human premotor cortex. Neuron *54*, 479–490.
21. Beaulieu, C. (2002). The basis of anisotropic water diffusion in the nervous system - a technical review. NMR Biomed. *15*, 435–455.
22. Basser, P.J., Mattiello, J., and LeBihan, D. (1994). Estimation of the effective self-diffusion tensor from the NMR spin echo. J. Magn. Reson. B. *103*, 247–254.
23. Basser, P.J., and Pierpaoli, C. (1996). Microstructural and physiological features of tissues elucidated by quantitative-diffusion-tensor MRI. J. Magn. Reson. B. *111*, 209–219.
24. Johansen-Berg, H., and Behrens, T.E. (2006). Just pretty pictures? What diffusion tractography can add in clinical neuroscience. Curr. Opin. Neurol. *19*, 379–385.
25. Klingberg, T., Hedehus, M., Temple, E., Salz, T., Gabrieli, J.D., Moseley, M.E., and Poldrack, R.A. (2000). Microstructure of temporo-parietal white matter as a basis for reading ability: Evidence from diffusion tensor magnetic resonance imaging. Neuron *25*, 493–500.
26. Head, D., Buckner, R.L., Shimony, J.S., Williams, L.E., Akbudak, E., Conturo, T.E., McAvoy, M., Morris, J.C., and Snyder, A.Z. (2004). Differential vulnerability of anterior white matter in nondemented aging with minimal acceleration in dementia of the Alzheimer type: Evidence from diffusion tensor imaging. Cereb. Cortex *14*, 410–423.
27. Smith, S.M., Jenkinson, M., Johansen-Berg, H., Rueckert, D., Nichols, T.E., Mackay, C.E., Watkins, K.E., Ciccarelli, O., Cader, M.Z., Matthews, P.M., and Behrens, T.E. (2006). Tract-based spatial statistics: Voxelwise analysis of multi-subject diffusion data. Neuroimage *31*, 1487–1505.
28. Eacott, M.J., and Gaffan, D. (1992). Inferotemporal-frontal disconnection: The uncinate fascicle and visual associative learning in monkeys. Eur. J. Neurosci. *4*, 1320–1332.
29. Mechelli, A., Friston, K.J., Frackowiak, R.S., and Price, C.J. (2005). Structural covariance in the human cortex. J. Neurosci. *25*, 8303–8310.
30. Lerch, J.P., Worsley, K., Shaw, W.P., Greenstein, D.K., Lenroot, R.K., Giedd, J., and Evans, A.C. (2006). Mapping anatomical correlations across cerebral cortex (MACACC) using cortical thickness from MRI. Neuroimage *31*, 993–1003.
31. Behrens, T.E., Berg, H.J., Jbabdi, S., Rushworth, M.F., and Woolrich, M.W. (2007). Probabilistic diffusion tractography with multiple fibre orientations: What can we gain? Neuroimage *34*, 144–155.
32. Toosy, A.T., Ciccarelli, O., Parker, G.J., Wheeler-Kingshott, C.A., Miller, D.H., and Thompson, A.J. (2004). Characterizing function-structure relationships in the human visual system with functional MRI and diffusion tensor imaging. Neuroimage *21*, 1452–1463.
33. Tuch, D.S., Salat, D.H., Wisco, J.J., Zaleta, A.K., Hevelone, N.D., and Rosas, H.D. (2005). Choice reaction time performance correlates with diffusion anisotropy in white matter pathways supporting visuospatial attention. Proc. Natl. Acad. Sci. USA *102*, 12212–12217.
34. Rushworth, M.F., Behrens, T.E., and Johansen-Berg, H. (2006). Connection patterns distinguish 3 regions of human parietal cortex. Cereb. Cortex *16*, 1418–1430.
35. Takahashi, M., Hackney, D.B., Zhang, G., Wehrli, S.L., Wright, A.C., O'Brien, W.T., Uematsu, H., Wehrli, F.W., and Selzer, M.E. (2002). Magnetic resonance microimaging of intraaxonal water diffusion in live excised lamprey spinal cord. Proc. Natl. Acad. Sci. USA *99*, 16192–16196.
36. Finsterer, J., and Fuglsang-Frederiksen, A. (2000). Concentric needle EMG versus macro EMG I. Relation in healthy subjects. Clin. Neurophysiol. *111*, 1211–1215.
37. Nandedkar, S., and Stalberg, E. (1983). Simulation of macro EMG motor unit potentials. Electroencephalogr. Clin. Neurophysiol. *56*, 52–62.
38. Tuch, D.S., Wedeen, V.J., Dale, A.M., George, J.S., and Belliveau, J.W. (2001). Conductivity tensor mapping of the human brain using diffusion tensor MRI. Proc. Natl. Acad. Sci. USA *98*, 11697–11701.
39. Haueisen, J., Tuch, D.S., Ramon, C., Schimpf, P.H., Wedeen, V.J., George, J.S., and Belliveau, J.W. (2002). The influence of brain tissue anisotropy on human EEG and MEG. Neuroimage *15*, 159–166.
40. Mills, K.R. (1999). Magnetic Stimulation of the Human Nervous System (New York: Oxford University Press).
41. Juraska, J.M., and Kopcik, J.R. (1988). Sex and environmental influences on the size and ultrastructure of the rat corpus callosum. Brain Res. *450*, 1–8.
42. Demerens, C., Stankoff, B., Logak, M., Anglade, P., Allinquant, B., Couraud, F., Zalc, B., and Lubetzki, C. (1996). Induction of myelination in the central nervous system by electrical activity. Proc. Natl. Acad. Sci. USA *93*, 9887–9892.